Catalysis of RNA Cleavage by a Ribozyme Derived from the Group I Intron of *Anabaena* Pre-tRNA^{Leu} †

Arthur J. Zaug, Jennifer A. Dávila-Aponte,‡ and Thomas R. Cech*

Howard Hughes Medical Institute, Department of Chemistry and Biochemistry, University of Colorado, Boulder, Colorado 80309-0215

Received September 6, 1994®

ABSTRACT: In the cyanobacterium *Anabaena* PCC7120, the precursor to tRNA^{Leu} contains a 249-nucleotide group I intron that undergoes efficient self-splicing in vitro. By deleting the 5′ and 3′ splice sites, this intron has now been converted to an RNA enzyme that uses a guanosine nucleophile to cleave substrate RNAs (S) with multiple turnover. This *Anabaena* ribozyme has a second-order rate constant for RNA cleavage $(k_{cat}/K_m)^S$ that is 250−500-fold smaller than that of the *Tetrahymena* ribozyme, and a multipl-turnover rate constant at saturating S $[k_{cat}(mt)]$ that is ~400-fold larger. Several lines of evidence, including kinetic analysis of cleavage of phosphorothioate- and deoxynucleotide-substituted substrates and pH dependence, support the conclusion that both $(k_{cat}/K_m)^S$ and $k_{cat}(mt)$ are limited by the actual chemical cleavage step. In contrast, for the *Tetrahymena* ribozyme, it has been shown that neither of these rate constants reflects the chemical step. These kinetic differences are expected from the shorter guide sequence−substrate pairing of the *Anabaena* ribozyme; for example, weaker binding of RNA speeds product release during multiple turnover and thereby overcomes the rate-limiting product release observed for the *Tetrahymena* ribozyme. Thus, the large kinetic differences represent superficial rather than fundamental differences between these ribozymes. Furthermore, the strength of the guanosine-binding interaction, the stereospecificity for R_P-phosphorothioate at the cleavage site, and the 10^3-fold slower cleavage with a deoxyribonucleoside leaving group are properties conserved between the *Anabaena* and *Tetrahymena* ribozymes. Finally, $\log(k_{cat}/K_m)^S$ increases linearly with pH in the acid range where chemistry is rate-limiting and becomes pH-independent above pH 7, perhaps because a conformational step becomes rate-limiting; again, these are characteristics shared with the *Tetrahymena* ribozyme. We conclude that two group I ribozymes, although differing in the identity of many of their active site nucleotides, nevertheless provide functionally similar active sites for sequence-specific RNA cleavage.

This is a study in phylogenetic chemistry: the analysis of functionally similar biological catalysts from phylogenetically distant sources, and the comparison of the chemical details of their catalytic mechanisms. The biocatalysts are group I ribozymes, RNA catalysts whose biological function is to perform RNA self-splicing.

Group I introns are widespread in nature, occurring in the nuclear, mitochondrial, and chloroplast genomes of eukaryotes as well as in eubacteria and their phage. They are defined by their conserved secondary structure, which includes a series of paired (helical) regions designated P1−P9 (Davies et al., 1982; Michel et al., 1982). Their mechanism of splicing involves two transesterification reactions; the first is initiated by an exogenous guanosine nucleophile, which cleaves at the 5′ splice site, while the second results in ligation of the flanking exons and excision of the intron (Cech et al., 1981; Zaug & Cech, 1982). The active site for RNA splicing is provided by the folded structure of the RNA itself (Kruger et al., 1982).

Group I introns were recently discovered in tRNA^{Leu} genes in *Anabaena* and other cyanobacteria by Kuhsel et al. (1990) and Xu et al. (1990). The *Anabaena* intron (Figure 1) is small in size, missing peripheral helices found in the well-studied introns of *Tetrahymena* (P5abc) and bacteriophage T4 (P7.1 and 7.2); these peripheral elements greatly stabilize the introns in which they are found (Doudna & Szostak, 1989; Beaudry & Joyce, 1990; van der Horst et al., 1991). Furthermore, the P1 duplex, which consists of the last few nucleotides of the 5′ exon paired to the internal guide sequence of the intron (Davies et al., 1982), is unusually short in the *Anabaena* intron, with only 3 base pairs preceding the 5′ splice site. For comparison, the *Tetrahymena* intron has 6 base pairs preceding its 5′ splice site. Nevertheless, the *Anabaena* intron is an efficient self-splicer, with maximum reaction rate and guanosine concentration dependence comparable to those of the *Tetrahymena* intron (Zaug et al., 1993; Xu et al., 1990). It was therefore of interest to further dissect the catalytic activity of the intron into its individual steps, to see how the structural differences influence the reactivity.

The *Tetrahymena* intron has been converted into a multiple-turnover ribozyme, able to cleave exogenous RNA substrates in a reaction analogous to the first step of RNA splicing (Zaug et al., 1986, 1988). The individual equilibrium constants and rate constants for substrate binding, the chemical cleavage step, and product release have been

† This work was supported by NIH Grant GM28039 to T.R.C. T.R.C. is an Investigator and A.J.Z. is a Senior Associate of the Howard Hughes Medical Institute. We thank the W. M. Keck Foundation for support of RNA science on the Boulder campus.

* To whom correspondence should be addressed.

‡ Present address: MSU−DOE Plant Research Laboratory, Michigan State University, East Lansing, MI 48824.

® Abstract published in *Advance ACS Abstracts,* November 15, 1994.

0006-2960/94/0433-14935$04.50/0 © 1994 American Chemical Society

determined (Herschlag & Cech, 1990a,b; Herschlag et al., 1991, 1993a,b; Pyle et al., 1992). This approach has continued to be mechanistically informative, revealing such features as two-step binding of oligonucleotide substrates [base-pairing to the internal guide sequence (IGS)[1] to form P1, followed by docking of P1 into the catalytic core (Herschlag, 1992; Bevilacqua et al., 1992)] and energetic coupling between RNA binding and guanosine binding (McConnell et al., 1993; Bevilacqua et al., 1993). It also proved to be invaluable for the correct interpretation of the phenotypes of site-specific mutants of the ribozyme (Young et al., 1991). Additionally, a kinetic framework for the hammerhead ribozyme has been presented (Fedor & Uhlenbeck, 1992; Hertel et al., 1994), and one is being developed for a bipartite form of the group II intron (Pyle & Green, 1994).

We now describe the conversion of the *Anabaena* self-splicing intron into a multiple-turnover ribozyme analogous to the L-21 *Sca*I form of the *Tetrahymena* ribozyme. We find that this L-8 HH *Anabaena* ribozyme[1] cleaves a cognate RNA substrate, S, with multiple turnover ~400 times faster than the *Tetrahymena* (*Tet*) ribozyme, and shows a different rate-limiting step (chemical step instead of product release). In contrast, under single-turnover conditions with subsaturating S [$(k_{cat}/K_m)^S$ conditions], the *Anabaena* ribozyme is several hundred times slower than the *Tet* ribozyme, again with a different rate-limiting step (chemical step instead of substrate binding). We argue that these kinetic differences are to be expected from the weaker binding of RNA substrate by the *Anabaena* ribozyme, which involves a 3 base pair IGS−substrate duplex (P1) instead of the 6 base pair P1 of the *Tet* ribozyme. In fact, many of the active site interactions appear fundamentally similar between these two group I ribozymes.

MATERIALS AND METHODS

Plasmid Construction. All constructs were made using oligonucleotide-directed mutagenesis (Kunkle, 1987). DNA oligonucleotides were synthesized on Thelma, an Applied Biosystems 380B DNA synthesizer, phosphorylated using ATP and polynucleotide kinase (NEB), and subsequently annealed to deoxyuridine-containing single-stranded circular DNA. Second-strand synthesis was accomplished by the addition of dNTPs, T4 DNA polymerase and T4 DNA ligase (both from U.S. Biochemical Corp.). Resultant double-stranded DNA was used to transform competent *Escherichia coli* JM109 using a Bio-Rad gene pulser set at 1.8 kV and 400 Ω. Plasmids were screened using restriction endonuclease digestion and sequencing (U.S. Biochemical Corp. Sequenase kits), and for the final constructs, the sequence of the entire intron was confirmed.

Genomic clone pXAb-107 was a gift from David Shub, and was constructed by inserting a 1.2 kb *Hin*dIII genomic fragment which contained the leucine tRNA gene from *Anabaena* PCC7120 into the *Hin*dIII site of pBS(−) (Stratagene) in the T7 promoter orientation. Construction of pAL-8, the plasmid that encodes the enzyme form of the group I intron, involved deleting 911 base pairs of pXAb-107 between the T7 promoter and the first base pair of the internal guide sequence of the intron. The sequence of the nontemplate strand at the promoter/+1 base of the transcript is TAATACGACTCACTATA/GAGCCTTA. In addition, an *Ear*I restriction endonuclease recognition site was inserted just beyond the 3′ end of the intron to allow linearization of the plasmid, thereby providing a termination site for transcription. Transcription of the resultant plasmid produces RNA that begins at nucleotide 9 of the intron and is predicted to end at nucleotide 248, one base before the terminal guanosine of the intron. This ribozyme is called L-8 *Ear*I. To provide a more uniform 3′ terminus, we designed another L-8 ribozyme that utilizes a hammerhead self-cleaving domain to process the 3′ end (Grosshans & Cech, 1991). Construction of pAL-8 HH involved adding a 46 base pair hammerhead cleavage domain near the 3′ end of the intron. In addition, a *Sma*I site was introduced just downstream from the hammerhead domain to allow linearization of the plasmid. In order to satisfy the requirements for the sequence preceding a hammerhead cleavage site (UX, where X = A, C, or U), the terminal guanosine of the intron was changed to an adenosine. After hammerhead self-cleavage, the L-8 HH ribozyme ends with an adenosine 2′,3′-cyclic phosphate at position 249 (Figure 1).

Transcription of L-8 EarI and L-8 HH Ribozymes. Transcription reactions, typically 1 or 2 mL, contained 40 mM Tris-HCl (pH 7.5), 15 mM $MgCl_2$, 10 mM DTT, 2 mM spermidine, 1 mM each NTP, 5 μg/mL DNA template (cleaved with *Ear*I for the L-8 *Ear*I ribozyme or with *Sma*I for the L-8 HH ribozyme), and 50 000 units/mL T7 RNA polymerase (activity determined relative to polymerase from the U.S. Biochemical Corp.). T7 RNA polymerase was purified from *E. coli* strain BL21 containing the plasmid pAR1219 (Davanloo et al., 1984). After the addition of polymerase, the mixture was incubated at 37 °C for 1 h. (No additional incubation was necessary for 3′-processing by the hammerhead motif of the L-8 HH ribozyme.) Transcription was stopped by the addition of 20 mM EDTA and 0.25 M NaCl, and RNA was precipitated by the addition of 3 volumes of ethanol. RNA was purified by electrophoresis on a 6% polyacrylamide [29:1, acrylamide:bis-(acrylamide) ratio]/8 M urea gel. The gel slice containing the RNA was crushed and soaked in 0.01 M Tris-HCl (pH 7.5), 0.001 M EDTA, and 0.25 M NaCl, followed by removal of the polyacrylamide by filtration and precipitation of RNA with ethanol. Purified ribozyme was dissolved in H_2O and quantitated spectrophotometrically (assuming 1 OD_{260} = 40 μg/mL, and the molecular weight of the ribozyme ≃79 200).

[1] Abbreviations: L-8 HH ribozyme, a catalytic RNA engineered from the *Anabaena* intron by deleting 8 nucleotides from its 5′ end and forming a discrete 3′ end by cleavage of a hammerhead ribozyme encoded by the same transcription unit; L-8 *Ear*I ribozyme, a catalytic RNA engineered from the *Anabaena* intron by deleting 8 nucleotides from its 5′ end and forming a 3′ end by runoff transcription from an *Ear*I-cleaved DNA template; L-21 *Sca*I ribozyme (*Tet* ribozyme), a catalytic RNA engineered from the *Tetrahymena* intron by deleting 21 nucleotides from its 5′ end and forming a 3′ end by runoff transcription from a *Sca*I-cleaved DNA template; IGS, internal guide sequence; P1, paired (duplex) region consisting of the IGS base-paired to the RNA undergoing cleavage; P2 through P9, additional paired regions conserved among group I introns; E, ribozyme; G, guanosine; pG, guanosine 5′-monophosphate; S, oligoribonucleotide substrate; Sd1, oligonucleotide substrate containing a single deoxynucleotide at the cleavage site; P, oligonucleotide representing the 5′-terminal product of ribozyme-catalyzed cleavage; k_c, single-turnover rate constant for conversion of E·G·S→products, the presumed chemical step; k_{cat}(mt), rate constant for RNA cleavage under multiple-turnover conditions with saturating S and G.

Oligonucleotide Substrates. Oligoribonucleotide substrates were synthesized on Louise, an Applied Biosystems 394 DNA/RNA synthesizer. Deprotection proceeded in concentrated NH_4OH/ethanol (3:1) overnight at 55 °C, after which the NH_4OH/ethanol solution was removed by vacuum. The silyl protecting groups were removed with 40 equiv of tetrabutylammonium fluoride (TBAF) per equivalent of silyl group for 16 h at room temperature in the dark. [In a typical 1 μmol synthesis of an 8mer (CUUAAAAA), 400 μL of 1 M TBAF in THF was used.] The mixture was then diluted with 1.2 mL of 0.01 M Tris-HCl (pH 7.5)/0.001 M EDTA. After the addition of NaCl to a final concentration of 0.5 M, 3 volumes of ethanol were added, and the mixture was placed at −20 °C for 1 h. The resultant precipitate was pelleted, dried, dissolved in 100 μL of H_2O, and quantitated spectrophotometrically.

In a typical labeling reaction, 25 pmol of oligonucleotide was phosphorylated in 10 μL of 70 mM Tris-HCl (pH 7.5), 10 mM $MgCl_2$, 5 mM DTT, 25 pmol of [γ-^{32}P]ATP (New England Nuclear), and 10 units of T4 polynucleotide kinase (New England Biolabs). After 30 min at 37 °C, the oligonucleotide was separated from unincorporated ATP by electrophoresis on a 20% polyacrylamide [29:1, acrylamide: bis(acrylamide) ratio]/8 M urea gel, and the gel slice containing the oligonucleotide was soaked in H_2O. Due to the small size of the oligonucleotide, precipitation with ethanol was inefficient following gel purification. Therefore, to remove the urea and salts, the oligonucleotide was absorbed to a C-18 Sep-pak column (Waters; prewashed with 5 mL of 40% CH_3CN/H_2O followed by 5 mL of H_2O). The oligonucleotide was eluted with 40% CH_3CN in H_2O. The CH_3CN was removed by vacuum, and the labeled oligonucleotide was used in subsequent kinetic studies.

Kinetics. All reactions were carried out at 32 °C in 25 mM Hepes (pH 7.5) and 15 mM $MgCl_2$ unless otherwise indicated. Prior to the addition of the oligonucleotide substrate, the ribozyme was preincubated in the presence of 25 mM Hepes (pH 7.5)/15 mM $MgCl_2$ with or without guanosine at 50 °C for 15 min followed by a 2 min incubation at 32 °C. Reactions were initiated by the addition of oligonucleotide substrate (preincubated at 32 °C). Typically, 3 μL portions were removed at specified times and stopped by adding to 3 μL of stop buffer consisting of 30 mM EDTA, 10 M urea, 0.01% bromophenol blue, 0.025% xylene cyanol, and 0.1 × TBE electrophoresis buffer (1 × TBE is 0.1 M Tris base, 0.083 M boric acid, and 1 mM EDTA). Typically, 6−8 time points were taken for a 60 min reaction. Reaction products were separated by electrophoresis on 20% polyacrylamide [29:1, acrylamide:bis-(acrylamide) ratio]/8 M urea gels, and the ratio of substrate to product was quantitated with the use of an AMBIS scanner or a Molecular Dynamics PhosphorImager. Reactions proceeded essentially to completion, typically with only 2−3% unreactive S; correction of the data for this end point did not change the values of the kinetic parameters, so the data shown herein are all uncorrected. At high [E], the concentration of ribozyme phosphate approaches that of Mg^{2+} in solution. Thus, it seemed possible that the saturation behavior observed in Michaelis−Menten plots might represent partial inactivation of the ribozyme due to chelation of Mg^{2+} by the RNA. However, kinetic analysis of the cleavage of S and Sd1 at 100 mM $MgCl_2$ showed that 15 mM $MgCl_2$ was sufficient for activity (A.J.Z. and T.R.C., unpublished).

Stability of the Ribozyme under Reaction Conditions. In anticipation of the long reaction times that would be required to cleave a 2′-deoxy-substituted substrate, the stability of the L-8 HH ribozyme after prolonged incubation was determined. The ribozyme (5 μM) was incubated for 20 h at 32 °C in reaction solution, and its activity was then compared side-by-side with a sample of ribozyme that had been incubated for the standard 2 min. The two preparations showed indistinguishable values of $(k_{cat}/K_m)^S$. Because the rate of cleavage in such single-turnover kinetic experiments is proportional to the concentration of active ribozymes, it could be concluded that the ribozyme activity was unaffected by 20 h incubation.

Uncertainty in Values of Kinetic Parameters. Estimation of error limits for rates of ribozyme-catalyzed RNA cleavage assayed by gel electrophoresis is as discussed previously (Herschlag & Cech, 1990a). In brief, rate constants for reactions performed side-by-side are precise to within 20%, and usually much better. However, experiments performed with different solutions on different days sometimes show greater variation, as large as 2-fold. When error limits are explicitly given in the text, they are based on goodness-of-fit of the data points to a straight line or to the Michaelis−Menten equation, and they do not take into account the possible 2-fold variation between the independent experiments.

Pulse−Chase Experiments. L-8 HH ribozyme (150 μM) in a volume of 2.5 μL was preincubated for 15 min at 50 °C, followed by 2 min at 32 °C as described above. ^{32}P-CUUAAAAA (2.5 μL) was added to each reaction, decreasing the concentration of the L-8 HH ribozyme to 75 μM and introducing a trace amount (2 × 10^6 cpm) of RNA substrate. After binding of substrate to the ribozyme for 0.5 min, the reaction was diluted 200-fold with buffer (±2 mM G). This dilution decreased the L-8 HH ribozyme concentration to 0.375 μM. In some experiments, 100 μM unlabeled S was added during the chase. Time points were taken and analyzed as described under Kinetics.

RESULTS

Conversion of the Intron into an RNA Enzyme. To engineer an RNA enzyme from the self-splicing *Anabaena* intron, the general approach used to develop the *Tetrahymena* L-21 ribozyme was followed (Zaug et al., 1986, 1988). The 5′ exon and the first 8 intron nucleotides were deleted by placing the promoter for T7 RNA polymerase such that transcription began with G9 of the intron. The resulting L-8 (a linear RNA minus 8 nucleotides) ribozyme has the IGS immediately at its 5′ end. Two methods were used to eliminate the 3′ splice site. In the first, an *Ear*I restriction endonuclease recognition site was introduced into the DNA template past the 3′ end of the intron, such that transcription from an *Ear*I-cleaved template would be expected give an RNA terminating with U248. The resulting RNA is termed the L-8 *Ear*I ribozyme. Runoff transcription usually gives RNA with limited heterogeneity at its 3′-terminus, including addition of nonencoded nucleotides (Milligan et al., 1987). Because 3′-terminal G residues are active in group I intron reactions, even when located at positions internal to the normal 3′ end of the intron (Joyce & Inoue, 1987; Grosshans & Cech, 1991), a second construct was made in which a hammerhead ribozyme (Symons, 1992) was included in the

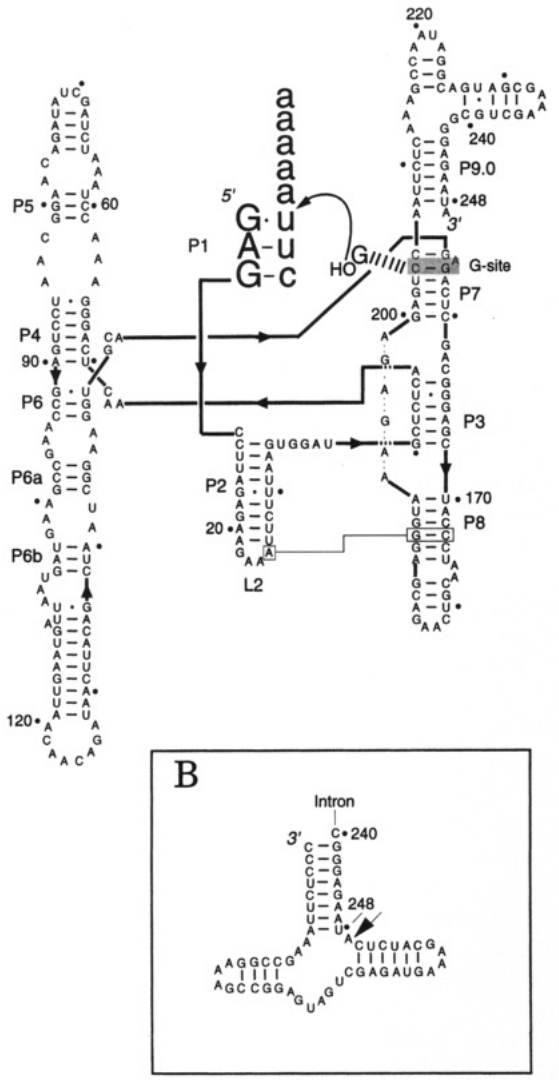

FIGURE 1: *Anabaena* PCC7120 group I ribozyme. (A) The L-8 HH ribozyme, which is missing the first eight nucleotides of the intron and has the 3′-terminal G changed to an A. It binds an RNA substrate (lower case letters), forming the P1 duplex, and cleaves this substrate by transesterification utilizing an exogenous guanosine nucleophile (G_{OH}). The self-splicing intron (not shown) is similar, but the 5′ exon (5′-cuu) is covalently joined to the internal guide sequence (5′-GAG) by a linker (5′-cuuAAAUAAUUGAG...; linker is underlined). Secondary structure format (Salvo & Belfort, 1992; Saldanha et al., 1993; Cech et al., 1994) emphasizes the P1 helix docked in an active site comprised of two RNA domains. Boldface lines represent connectivity of RNA (no nucleotides have been omitted), and arrowheads give 5′ → 3′ directionality. P1 is thought to be coaxially stacked on P2, with the GAAA tetraloop (L2) forming a tertiary interaction with P8 to help position P1 for cleavage (Michel & Westhof, 1990). (B) The hammerhead ribozyme that was engineered into the primary transcript; self-cleavage at the position shown by the arrow produces the L-8 HH *Anabaena* ribozyme, terminating at A249 with a 2′,3′-cyclic phosphate.

primary transcript (Figure 1B). Self-cleavage then produces a 3′ end that is essentially homogeneous (Grosshans & Cech, 1991). Furthermore, the 2′,3′-cyclic phosphate terminus left by hammerhead cleavage is blocked for further transesterification reactions. We term this the L-8 HH ribozyme (Figure 1A).

Either the L-8 *Ear*I or the L-8 HH ribozyme was incubated with radiolabeled oligonucleotide substrate under conditions

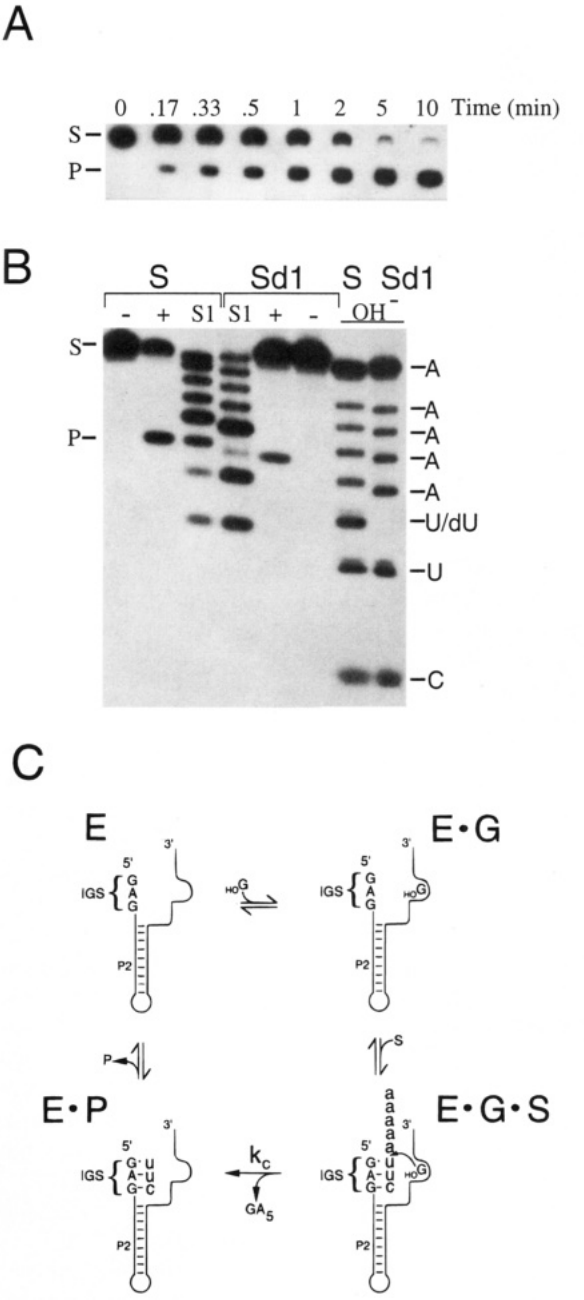

FIGURE 2: RNA cleavage catalyzed by the L-8 *Anabaena* ribozyme. (A) Cleavage of 5′-^{32}P end-labeled CUUAAAAA substrate (S) with 2 mM guanosine and excess ribozyme (2.5 μM) at 32 °C. Portions of the reaction mixture were removed at the indicated times, stopped, and analyzed by polyacrylamide gel electrophoresis. (B) Cleavage occurs after CUU. The 5′-labeled all-ribo substrate (S) and the substrate with a single deoxynucleotide at the cleavage site (Sd1) were analyzed on a 20% polyacrylamide gel without reaction (−), after reaction with ribozyme and guanosine (+), or after partial digestion with S1 nuclease (S1). S1 nuclease cleaves after both ribo- and deoxyribonucleotides, leaving a 3′-OH terminus, the same terminus left by ribozyme cleavage. The fastest-migrating species on the S1 ladder is pC. Substrates were also partially hydrolyzed by alkali (OH^-), which leaves a 3′-phosphate terminus and reveals the position of deoxy-substitution as a gap. The fast-migrating species on the OH^- ladder is pCp. (C) Pathways for binding and cleavage of S by guanosine (G_{OH}) catalyzed by the *Anabaena* ribozyme (E).

that had previously been used to study *Anabaena* tRNA self-splicing. Reactions included guanosine (G) as the nucleophile in the transesterification reaction. As shown in Figure 2A,B, the substrate was cleaved at a single site, CUU/AAAAA, which is the same internucleotide linkage that

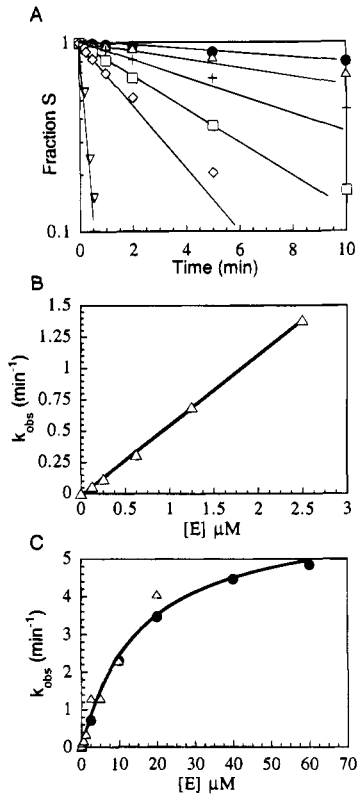

FIGURE 3: Single-turnover reactions as a function of ribozyme concentration. (A) Semi-log plot showing the disappearance of RNA substrate with time at increasing L-8 *Ear*I ribozyme concentrations of (●) 0.125, (△) 0.25, (+) 0.626, (□) 1.25, (◇) 2.5, and (▽) 20 μM. Observed values of $[S]_t/([S]_t + [P]_t)$, uncorrected for the end point of unreactive substrate (see Materials and Methods), are plotted *vs t*. Each reaction contained 15 mM $MgCl_2$, 25 mM Hepes (pH 7.5), and 2.0 mM guanosine. The reaction was initiated by the addition of a trace amount of ^{32}P-labeled CUUAAAAA and proceeded at 32 °C. (B) k_{obs}, determined from the slope of each line in (A) (0.125−2.5 μM), is plotted vs ribozyme concentration, [E]. The resulting line has slope = $(k_{cat}/K_m)^S = 5.6 \times 10^5$ M^{-1} min^{-1}. (C) Determination of K_m^S for the L-8 HH ribozyme. Different symbols represent independent experiments. The line is the least-squares fit to the Michaelis−Menten equation ($k_{cat} = 6.3 \pm 0.4$ min^{-1}; $K_m = 15 \pm 2$ μM).

forms the 5′ splice site for self-splicing. Such cleavage involves a number of steps, including binding of G and of the RNA substrate, the chemical step, and product release (Figure 2C). The remainder of this paper will describe kinetic experiments used to determine the rates of the individual steps that comprise this catalytic cycle.

Reaction of the Ribozyme with Its RNA Substrate. Single-turnover reactions in excess ribozyme were used to evaluate the reaction of the ribozyme with its RNA substrate in the presence of saturating guanosine. Under such conditions, the rate-limiting step is likely to be the chemical cleavage step or some step that precedes chemistry, such as RNA binding. [Only if both products were released slowly, such that there was a significant reverse reaction on the ribozyme, would the rate of product release affect the single-turnover rate. Arguments against this possibility have been presented by Herschlag and Cech (1990a) for the *Tet* ribozyme.]

The conversion of S (the RNA substrate) to P (the 5′-labeled cleavage fragment) followed pseudo-first-order kinetics (Figure 3A). The rate, determined from the slope of each time course, increased linearly with L-8 *Ear*I ribozyme concentration (Figure 3B), demonstrating that E was not saturated with S throughout the range tested. (Thus, $K_m^S > 2.5$ μM and $k_{cat} > 1.5$ min^{-1}.) The apparent second-order rate constant for reaction of E·G with S was calculated from the slope of the line in Figure 3B: $(k_{cat}/K_m)^S = k_{obs}/[E] = 5.6 \times 10^5$ M^{-1} min^{-1}. A measurement by a different coauthor using an independent preparation of ribozyme gave $(k_{cat}/K_m)^S = 5.1 \times 10^5$ M^{-1} min^{-1}. (The uncertainty associated with all kinetic values described herein is discussed under Materials and Methods.) The same experiment performed with the L-8 HH ribozyme consistently gave a similar but slightly lower value, 2.9×10^5 M^{-1} min^{-1}.

When the concentration of the L-8 HH ribozyme was increased, saturation behavior was observed (Figure 3C). These data were well fit by the Michaelis−Menten equation, giving $k_{cat} = 6.3 \pm 0.4$ min^{-1} and $K_m = 15 \pm 2$ μM. The calculated $(k_{cat}/K_m)^S = 4 \times 10^5$ M^{-1} min^{-1} is in good agreement with the value of 2.9×10^5 M^{-1} min^{-1} obtained from the linear portion at low [E] (see above).

Each rate constant for the *Anabaena* ribozyme will be compared to that obtained previously for the *Tetrahymena* ribozyme under similar conditions. As shown in Table 1, $(k_{cat}/K_m)^S$ is about 500-fold greater for the *Tet* ribozyme. However, evidence will be presented below that this kinetic parameter does not represent the same elemental reaction step in the two cases.

Reaction of the Ribozyme with Its Guanosine Substrate. Single-turnover reactions were performed with increasing [G] at a ribozyme concentration that was subsaturating with respect to [S]. The resulting K_m^G therefore represents the apparent binding of G to free E, not to E·S. [It will equal K_m^G for the E·S complex only if binding of G and S are independent, an assumption which is likely to be a reasonable first-order approximation but to be inaccurate in detail (McConnell et al., 1993; Bevilacqua et al., 1993).] In these experiments, it was important to use the L-8 HH ribozyme, because at low [G] any 3′-terminal G-OH on the ribozyme itself begins to participate significantly in the reaction. Furthermore, guanosine 5′-monophosphate (pG) was used instead of guanosine, because of its higher solubility.

Table 1: Steady-State Kinetic Parameters for the *Anabaena* Ribozyme

kinetic parameter	*Anabaena* ribozyme[a]	self-splicing[b]	*Tetrahymena* ribozyme[c]
k_{cat} (min^{-1})	4 ± 2	14 ± 4	25
K_m^G (μM)	480 ± 120	240 ± 60	320 (E) 90 (E·S)
$(k_{cat}/K_m)^G$ (M^{-1} min^{-1})	~1 × 10^4	(4.6 ± 0.4) × 10^4	~3 × 10^5
K_m^S (μM)	15 ± 2	NA	0.0001[d]
$(k_{cat}/K_m)^S$ (M^{-1} min^{-1})	(2.9 ± 0.3) × 10^5	NA	1.4 × 10^8
k_{cat}(mt) (min^{-1})	4 ± 1	NA	~0.01

[a] Reaction is cleavage of pCUUAAAAA by G (or pG) in 15 mM $MgCl_2$/25 mM Hepes (pH 7.5) at 32 °C. All values were derived from single-turnover experiments except k_{cat}(mt), which is the multiple-turnover rate constant. All values are for the L-8 HH ribozyme except k_{cat}(mt), which utilized the L-8 *Ear*I ribozyme. For the L-8 *Ear*I ribozyme, $(k_{cat}/K_m)^S$ was 5.6 × 10^5 M^{-1} min^{-1}. [b] Step 1 of self-splicing of *Anabaena* pre-tRNA from Zaug et al. (1993). NA, not applicable because RNA "substrate" is covalently attached to the catalytic portion. [c] Reaction is cleavage of pCCCUCUAAAAA by pG in 10 mM $MgCl_2$/50 mM Mes (pH 7.0) at 30 °C by L-21 *Sca*I ribozyme from McConnell et al. (1993) or McConnell and Cech (unpublished data). [d] For the *Tet* ribozyme, $K_m^S \neq K_d^S$. Therefore, the value of K_d^S is listed to enable comparison of the equilibrium constants for substrate binding for the two ribozymes.

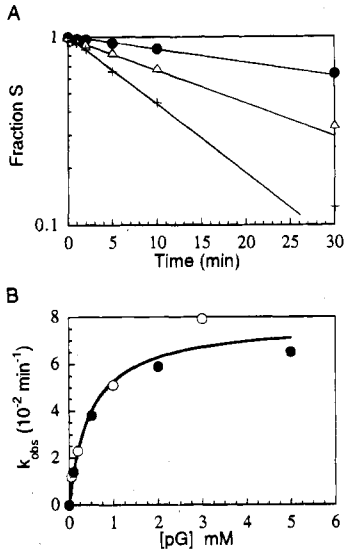

FIGURE 4: Determination of K_m for pG in single-turnover reactions. (A) Semi-log plot showing the disappearance of substrate with time at 2.5 μM L-8 HH ribozyme, a trace concentration of 5′-end-labeled pCUUAAAAA, and pG concentrations of (●) 0.1, (△) 0.5, and (+) 3.0 mM. (B) Plot of k_{obs} [from the slope of the lines in (A) plus equivalent data at additional pG concentrations] vs pG concentration. Open and filled symbols represent independent experiments. The line is the least-squares fit to the Michaelis–Menten equation, with k_{max} = 0.08 min^{-1} and K_m = 480 μM.

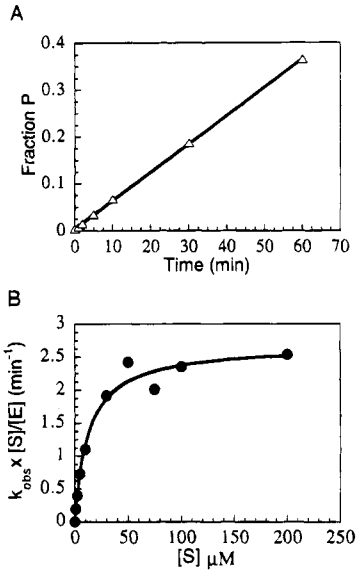

FIGURE 5: Multiple-turnover cleavage of RNA by the *Anabaena* ribozyme. (A) 50 μM S, 0.125 μM L-8 *Ear*I ribozyme, and 2.0 mM guanosine. Solution conditions as described in the legend to Figure 3. (B) k_{obs} was determined from the slopes of the linear least-squares fits to data such as those shown in (A). Plot of k_{obs}[S]/[E] vs [S]. The line is the best fit to the Michaelis–Menten equation [k_{cat}(mt) = 2.68 ± 0.12 min^{-1}; K_m = 13.1 ± 0.1 μM).

[Previous studies with the *Tet* ribozyme have shown G and pG to be essentially interchangeable (McConnell et al., 1993; T. S. McConnell and T. R. Cech, unpublished results).]

Reactions followed pseudo-first-order behavior (Figure 4A). When k_{obs} was plotted against [pG], saturation behavior was observed (Figure 4B). The derived K_m^G = 0.48 mM, similar to the K_m = 0.32 mM for pG binding to the free *Tetrahymena* ribozyme (Table 1).

In the multiple-turnover reactions described below, K_m^G for reaction of the E·S complex could be studied by using a saturating concentration of S. An estimate of K_m^G = 0.6 mM was based on kinetic analysis at 0.1, 0.5, and 2.0 mM pG (data not shown). The similarity of the values obtained for pG binding to E·S and to free E indicates that any energetic coupling between G and S binding is likely to be subtle.

Ribozyme-Catalyzed Cleavage in the Absence of Added G. Site-specific cleavage of S persisted at a low rate in the absence of added G. For the L-8 HH ribozyme $(k_{cat}/K_m)^S$ was 0.15 (±0.02) × 10^5 M^{-1} min^{-1}, 20-fold lower than the measurement with the same ribozyme preparation in the presence of 2 mM G. Group I introns and ribozymes derived therefrom are known to catalyze site-specific hydrolysis reactions, using OH^- or H_2O as the nucleophile (Zaug et al., 1984; Inoue et al., 1986; Kay & Inoue, 1987; Tanner & Cech, 1987; Herschlag & Cech, 1990a). We are therefore tempted to assign the reaction of the *Anabaena* ribozyme in the absence of added G as a hydrolysis reaction. However, we have not monitored the 3′-cleavage fragment (the one that would incorporate the nucleophile during the reaction), so it remains possible that GTP or other nucleotides might contaminate the ribozyme preparation and contribute to the reaction in the absence of added G. Thus, values reported for "−G" reactions in this paper represent upper bounds for hydrolysis rate constants.

Multiple-Turnover Reactions. When ribozyme was incubated in the presence of excess RNA substrate and saturating guanosine, reaction occurred with multiple turnover. For example, after 60 min in the reaction shown in Figure 5A, 0.125 μM ribozyme had cleaved 20 μM S, an average of 160 turnovers per ribozyme. The multiple-turnover reaction showed saturation behavior, with k_{cat}(mt) = 2.7 min^{-1} and K_m^S = 13 μM (Figure 5B).

Note that the multiple-turnover $(k_{cat}/K_m)^S$ = 2.7/(13 × 10^{-6}) M^{-1} min^{-1} = 2 × 10^5 M^{-1} min^{-1}, equal within a factor of 3 to the single-turnover value described above. Furthermore, k_{cat}(mt) (2.7, 3.7, 4.1 and 5.1 min^{-1} in four independent experiments) is equal within a factor of 2 to the single-turnover value of k_{cat} = 6.3 min^{-1} measured in a single experiment (Figure 3C). Considering the uncertainty inherent in such measurements (see Materials and Methods), the simplest interpretation is that k_{cat}(mt) is equal to k_{cat}. In addition, the multiple-turnover K_m of 13 μM (Figure 5B) is equal to the single-turnover K_m of 15 ± 2 μM (Figure 3C).

Comparison of these kinetic parameters with those measured for the *Tetrahymena* ribozyme reveals large differences (Table 1). The *Anabaena* ribozyme has a K_m^S (which is expected to equal K_d^S; see Discussion) that is 100 000-fold higher than K_d^S of the *Tet* ribozyme. Qualitatively, weaker binding is expected because the *Anabaena* E·S complex involves a smaller number of base pairs (3 base pairs compared to 6 in *Tetrahymena*). The *Anabaena* ribozyme has a k_{cat}(mt) that is ~400-fold faster than that of the *Tet* ribozyme, which is again in the direction expected: the *Tet* ribozyme is rate-limited by product release (Herschlag & Cech, 1990a,b), so the shorter base-pairing interaction in the *Anabaena* ribozyme would be expected to weaken binding of P. Because k_{cat} is the same for single-turnover and multiple-turnover reactions, it appears that product release is not rate-limiting for the *Anabaena* ribozyme reaction.

Model for the Reaction Free Energy Profile and Experimental Tests. For the *Tet* ribozyme under single-turnover

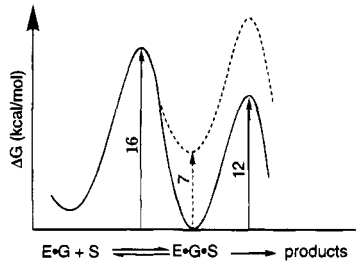

FIGURE 6: Free energy reaction profiles for cleavage of cognate RNAs by the *Anabaena* (dashed line) and *Tetrahymena* (solid line) ribozymes. Reaction with saturating G and subsaturating oligonucleotide substrate; i.e., "$(k_{cat}/K_m)^S$ conditions." The free energy profile is for [S] = 0.1 nM, [E] ≪ 0.1 nM, and [G] ≫ K_d^G, calculated as described by Young et al. (1991) from the rate and equilibium constants listed in Table 1. The numbers refer to free energy differences (kcal/mol). The height of the first energy barrier (for binding of S) for the *Anabaena* ribozyme has not been measured, but is shown as being equal to that for the *Tet* ribozyme on the basis of oligonucleotide hybridization studies (Turner et al., 1990).

conditions, $(k_{cat}/K_m)^S$ is limited by the rate of binding of the RNA substrate (k_{on}^S) (Herschlag & Cech, 1990a). The rates of formation of 3 bp duplexes, as would occur during substrate binding to the *Anabaena* ribozyme, are within the range of those determined for somewhat longer duplexes (Turner et al., 1990). Thus, the much lower value of $(k_{cat}/K_m)^S$ for the *Anabaena* ribozyme suggested that a step other than binding of S might have become rate-limiting. Furthermore, the weaker binding of S by the *Anabaena* ribozyme means that its E•S complex is destabilized by 7 kcal/mol relative to the same complex formed with the *Tet* ribozyme. Thus, it seemed plausible that the chemical step might now be the highest free-energy barrier along the reaction coordinate for the *Anabaena* ribozyme (Figure 6), unless its chemical step had become much *faster* than that of the *Tet* ribozyme. This latter possibility seems remote: $(k_{cat}/K_m)^G$, a parameter limited by the chemical step, is ~30-fold *slower* for the *Anabaena* ribozyme, and its K_m^G is similar, so k_c is calculated to be slower.

In the case of the *Tet* ribozyme, pulse−chase experiments (Rose et al., 1974) showed that >90% of the E•G•S ternary complexes formed went on to react rather than to dissociate (Herschlag & Cech, 1990a). That is, considering the solid line in Figure 6, the free energy barrier for dissociation is considerably higher than that for the chemical step. One prediction of the model for the *Anabaena* ribozyme (dashed line in Figure 6) is that E•G•S complexes would partition in the opposite direction, giving dissociation of S.

In the pulse−chase experiment, a high concentration of L-8 HH ribozyme was used to drive the formation of the E•S complex ([E] ≫ K_m^S; evidence that $K_m^S = K_d^S$ will be discussed below). The solution was then diluted 200-fold, such that [E] ≪ K_m^S. The diluent was buffer ± guanosine (2 mM), and cleavage of S was monitored as a function of time. The rate was compared to that of a parallel reaction which was not diluted. The rate of cleavage dropped dramatically upon dilution, indicating that dissociation of S from the E•S complex was very rapid. (In some experiments, 100 μM unlabeled S was added during the chase, but this was unnecessary to achieve an effective chase.) Because each graph of log(fraction unreacted) vs time showed simple linear decay (characterized by a single rate constant) with no apparent burst phase, the data are not shown but are instead summarized in Table 2. Reaction by guanosine or in the absence of G proceeded at a rate that was within a factor of 2 of that predicted for the concentration of E after dilution. If instead the chemical step had been the lower barrier, as in the case of the *Tet* ribozyme (Figure 6), the reaction kinetics after dilution would have been the same as in the undiluted sample. Thus, the E•S•G complex formed with the *Anabaena* ribozyme sees a lower activation energy barrier for dissociation than for progression to products.

Table 2: Pulse−Chase Experiment Provides Evidence That $k_{off} \gg k_c$

	k_{obs} (min^{-1})	
	+G	−G
observed at 75 μM E[a]	2.3	0.42
observed after 200 × dilution[b]	0.069	0.007
expected for 200 × dilution if $k_{off} \gg k_c$[c]	0.067	0.012

[a] The rate of cleavage of a trace amount of RNA substrate by the L-8 HH ribozyme was followed at high ribozyme concentration (75 μM) in the presence or absence of 2 mM guanosine (+G and −G, respectively; reaction in the absence of G occurs at the same site as the reaction by G, presumably by hydrolysis). Although both reactions gave good first-order plots, the reaction +G was so rapid that it could only be followed for three time points (15, 30, and 60 s) after which it was essentially complete, so this value may be less accurate. [b] The cleavage reaction was monitored as a function of time immediately after a 200-fold dilution with buffer (±2 mM G). [c] Calculated from the k_{obs} at 75 μM E, using K_m^S = 15 μM (Table 1) and assuming that S reequilibrates rapidly (i.e., $k_{off} \gg k_c$). If, on the other hand, $k_c \gg k_{off}$ as for the *Tet* ribozyme, then the rate observed after dilution should equal that at 75 μM E.

The pulse−chase experiment identifies the rate-limiting transition state as some step that follows formation of the E•S•G ternary complex, but this need not necessarily be the chemical step. There could, for example, be a rate-limiting conformational change of the E•S•G complex that was followed by a faster chemical step. The data presented in the next three sections provide strong evidence that the actual chemical step is at least partially rate-limiting.

Reactions with a Phosphorothioate at the Cleavage Site Reveal Stereospecificity and Help Identify the Chemical Step. Previous detailed studies with the *Tet* ribozyme provide a framework for interpreting the effects of thio substitution on cleavage rate, and will be briefly reviewed. Of the two diastereomers, only the R_P isomer is efficiently cleaved in the G-addition reaction; the S_P isomer is cleaved ~5000-fold more slowly (McSwiggen & Cech, 1989; Herschlag et al., 1991; T. S. McConnell, unpublished data). For the R_P isomer, the kinetic "thio-effect" (the ratio of the rate of cleavage of the phosphorothioate substrate to that of the normal all-oxygen substrate) is ~1 under conditions where the rate is determined by binding of S, and increases to 2.3 under conditions where the chemical step is rate-limiting (Herschlag et al., 1991). Such a modest thio-effect is expected for the intrinsic chemical reactivity of the phosphorothioate diester (Burgers & Eckstein, 1979; Herschlag et al., 1991), in contrast to the large intrinsic thio-effects seen for the triester (Benkovic & Schray, 1978).

To test cleavage by the *Anabaena* ribozyme, we chemically synthesized a chiral substrate (S_{thio}) with a single phosphorothioate linkage at the cleavage site. Such molecules are expected to be roughly equal mixtures of the two diastereomers, R_P and S_P. In a single-turnover reaction by

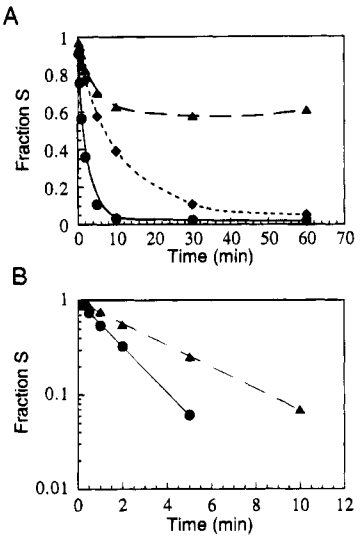

FIGURE 7: Cleavage shows stereospecificity for the R_P diastereomer. (A) Single-turnover reactions with 1.25 μM L-8 HH ribozyme, 2 mM guanosine, and trace amounts of three RNA substrates: (●) S; (▲) S_{thio}; and (♦) S(R_P). S_{thio} was chemically synthesized with a thiophosphate (mixture of R_P and S_P) at the cleavage site. S(R_P) was synthesized by transcription with ATPαS, so has the R_P diastereomer at the cleavage site and at the next four linkages in CUUAAAAA. (B) Semi-log plot of the data in (A), with the data for cleavage of S_{thio} renormalized to correct for 40% active substrate in the population [presumably the R_P subfraction, based on the fact that cleavage of S(R_P) proceeded essentially to completion].

the L-8 HH ribozyme (Figure 8A) or the L-8 *Ear*I ribozyme (data not shown), S_{thio} was quickly cleaved to 40% completion, the other 60% being resistant to cleavage even after 60 min. In contrast, the normal phosphate-containing S was cleaved to 95% completion. This was the behavior expected if only one of the two diastereomers was a good substrate.

To determine which diastereomer was active, a substrate was synthesized by transcription using phage T7 RNA polymerase and adenosine 5′-*O*-(1-thiotriphosphate) (ATPαS) (Milligan et al., 1987; McSwiggen & Cech, 1989). The polymerase uses only the S_P diastereomer of ATPαS and inverts it to the R_P isomer upon incorporation (Burgers & Eckstein, 1978; Griffiths et al., 1987). As shown in Figure 7A, this S(R_P) substrate was cleaved essentially to completion. [Its 3-fold reduced rate relative to the fast-reacting 40% of S_{thio} has not been further investigated, but may be due to the fact that S(R_P) contains an additional four phosphorothioates in its 3′AAAAA tail.] We conclude that the R_P diastereomer is the actively cleaved isomer, as in the case of the *Tet* ribozyme reaction.

The slower cleavage of the phosphorothioate-containing substrate relative to S (Figure 7B) was examined as a function of ribozyme concentration (Figure 8) to enable calculation of $(k_{cat}/K_m)^S$. For the reaction with guanosine, $(k_{cat}/K_m)^S = 5.1 \times 10^5$ M^{-1} min^{-1} (in good agreement with the independent value reported in Table 1) and $(k_{cat}/K_m)^{S_{thio}} = 2.5 \times 10^5$ M^{-1} min^{-1}. The thio-effect, calculated as the ratio of these two values, is 2.1. These results are summarized in Table 3, along with the thio-effect for the reaction in the absence of guanosine.

Reactions with a Deoxyribonucleotide at the Cleavage Site Confirm Identification of the Chemical Step. In the case of the *Tet* ribozyme, substitution of a single 2′-deoxynucleotide at the cleavage site decreases binding of an RNA substrate by only 3-fold but decreases the rate of the chemical step

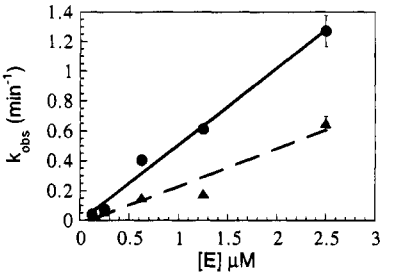

FIGURE 8: Thio-effect of ~2 in the presumed chemical step. (●) S; (▲) S_{thio}, the 40% that is reactive. Single-turnover reactions of the L-8 *Ear*I ribozyme with 2 mM guanosine. Each point comes from the slope of a time course similar to that shown in Figure 7B.

Table 3: Cleavage of a Substrate with a Single Phosphorothioate at the Cleavage Site

		Anabaena ribozyme[a]	*Tetrahymena* ribozyme[b]
+G	$(k_{cat}/K_m)^S$ (M^{-1} min^{-1})	$(5.1 \pm 0.4) \times 10^5$	
	$(k_{cat}/K_m)^{S_{thio}}$ (M^{-1} min^{-1})	$(2.5 \pm 0.2) \times 10^5$	
	thio-effect[c]	2.1 ± 0.3	2.3 ± 0.2
−G	$(k_{cat}/K_m)^S$ (M^{-1} min^{-1})	$(0.15 \pm 0.2) \times 10^5$	
	$(k_{cat}/K_m)^{S_{thio}}$ (M^{-1} min^{-1})	$(0.07 \pm 0.004) \times 10^5$	
	thio-effect[c]	2.2 ± 0.4	7 ± 2

[a] Data for cleavage of S_{thio} pertain to the 40% of the substrate that was cleaved. [b] From Herschlag et al. (1991). For the *Tet* ribozyme, $(k_{cat}/K_m)^S$ monitors substrate binding, not the chemical step, so the thio-effect on chemistry must be calculated from different kinetic parameters (see footnote *c*). [c] Determined as the ratio of the $(k_{cat}/K_m)^S$ values for the *Anabaena* ribozyme and as the ratio of the $(k_{cat}/K_m)^G$ values (+G) or of the k_c (−G) values for the *Tetrahymena* ribozyme.

Table 4: Cleavage of a Substrate with a Single Deoxynucleotide at the Cleavage Site[a]

	Sd1	S	S/Sd1
k_{cat} (min^{-1})	$(3.3 \pm 0.1) \times 10^{-3}$	6.3 ± 0.4	1900
K_m^S (μM)	15 ± 1	15 ± 2	1.0
$(k_{cat}/K_m)^S$ (M^{-1} min^{-1})	1.7×10^2	2.9×10^5	1700

[a] Data at pH 7.5. Note that k_{cat} and K_m^S were determined by fitting data similar to those shown in Figure 3C by the Michaelis−Menten equation; $(k_{cat}/K_m)^S$ was not determined by division, but from the slope of the graph of k_{obs} *vs* [E] as in Figure 3B, and was therefore determined independently of k_{cat} and K_m^S.

by 600-fold (Herschlag et al., 1993b; Herschlag & Khosla, 1994). Systematic variation of the pK_a of the leaving group has shown that the slower cleavage can be largely or entirely explained by the decreased chemical stability of the leaving group (Herschlag et al., 1993b). That is, the 3′-oxyanion of ribose is a poor leaving group (p$K_a \simeq 12.5$), but the 3′-oxyanion of 2′-deoxyribose is a much poorer leaving group (p$K_a \simeq 15-16$).

A deoxyribonucleotide-containing substrate, Sd1, was synthesized for the *Anabaena* ribozyme. Sd1 is identical to S except for the deoxyribonucleotide preceding the cleavage site: CU(dU)AAAAA. Single-turnover kinetic experiments were performed with 1−60 μM L-8 HH ribozyme. Long reaction times (1−24 h) were required, but the ribozyme retained full activity during these reactions (see Materials and Methods). Sd1 was cleaved at a single position, CU(dU)/AAAAA (Figure 2B), equivalent to the position of cleavage of the all-ribo substrate. The kinetic data (not shown) appeared very similar to those shown for the all-ribo substrate in Figure 3C, except that the maximum velocity was 1900 times lower. The Michaelis−Menten equation

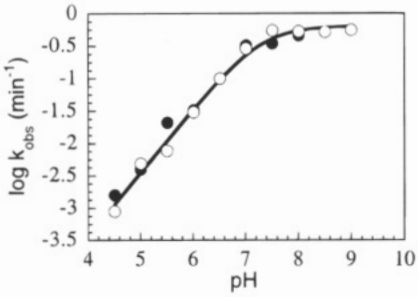

FIGURE 9: pH dependence of RNA cleavage measured in single-turnover reactions. Open and closed symbols represent different sets of experiments. The line, representing the best fit of the data to a simple titration curve, has slope = 1 in the acid range and an apparent pK_a = 7.3. Buffers were acetate (pH 4.5−5.5), Mes (pH 5.0−6.5), Hepes (pH 6.5−8.5), and Ches (pH 8.5−9.0).

gave an excellent fit to the data, resulting in the kinetic parameters summarized in Table 4. The 10^3-fold decrease in reaction rate upon deoxyribonucleotide substitution, with no effect on substrate binding, provides strong evidence that the kinetic parameters being measured are largely rate-limited by the chemical cleavage step.

pH Dependence. The chemical cleavage step of the *Tetrahymena* ribozyme reaction shows a log-linear increase in rate with pH in the acid range, consistent with deprotonation of a group (perhaps the 3′-OH of the G nucleophile) in the transition state (Herschlag et al., 1993a,b). In contrast, substrate binding, docking of the substrate−IGS helix (P1), and G binding are not pH-dependent in this same range (T. McConnell and T. R. Cech, unpublished results; D. Herschlag, personal communication). At pH >7, the rate of the *Tet* ribozyme reaction levels off, and good evidence has been presented that this represents a change in the rate-limiting step from the chemical step to a physical step, probably a conformational change (Herschlag & Khosla, 1994). Thus, pH dependence can provide another test for the identification of the chemical step in the *Anabaena* ribozyme reaction.

The pH dependence of $(k_{cat}/K_m)^S$ for the *Anabaena* ribozyme is shown in Figure 9. The $\log(k_{cat}/K_m)^S$ increases linearly with pH in the acid range, with a slope ≃1. At pH >7, the reaction rate levels off, becoming essentially pH-independent. These data could be explained by either of two models: (1) a titratable group with pK_a ≃ 7 is involved in the chemical step, or (2) there is a change in the rate-limiting step at pH ≃ 7. As an example of the second model, some pH-independent conformational step with an observed rate of 4 min^{-1} becomes rate-limiting at pH ≃7 and provides a "ceiling" for the reaction rate, even though the actual chemical step continues to increase in rate with pH.

To discriminate between these models, we adopted the technique of Herschlag and Khosla (1994), measuring the ratio of the rate of cleavage of S *vs* Sd1 as a function of pH. If model 1 were correct, the simplest expectation would be for the S/Sd1 cleavage ratio to remain constant throughout the pH range. (Only if the hypothetical titratable group were involved in stabilization of the leaving group *and* provided unequal stabilization to ribose *vs* deoxyribose leaving groups would the ratio change.) If model 2 were correct, the S/Sd1 cleavage ratio should be a constant value of ~10^3 in the pH range where the reaction rate increases linearly with [OH^-], and should converge to a small value when the other step such as a conformational change becomes rate-limiting. (A ratio = 1 would be expected if the new rate-limiting step were independent of the nature of the sugar adjacent to the cleavage site.)

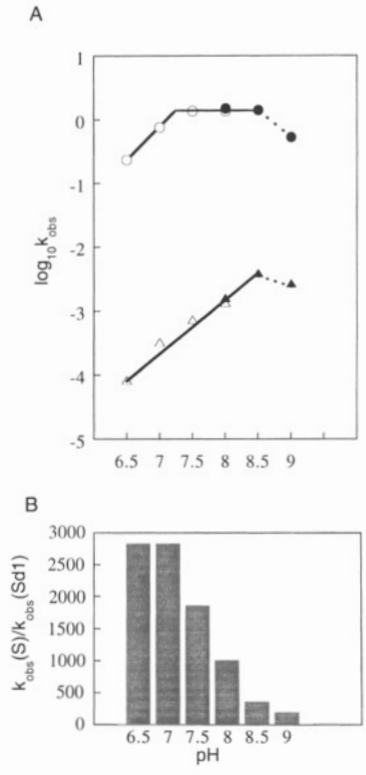

FIGURE 10: Cleavage of Sd1 as a function of pH. (A) Rate constants for the cleavage of (△) Sd1, which contains a single deoxynucleotide at the cleavage site, and (○) S. Open and filled symbols represent different sets of experiments. Filled symbols, preincubation at 50 °C (see Materials and Methods) was reduced from 15 to 5 min. (B) The ratio of the rate constants in (A). Single-turnover reactions were performed with 5 μM E and 2 mM G. Buffers were Hepes (pH 6.5, 7.0, 7.5, and 8.0) and Ches (pH 8.5 and 9.0).

The experimental results are summarized in Figure 10. The S/Sd1 cleavage ratio was 2800 at both pH 6.5 and pH 7.0, and then decreased at higher pHs. The results are very similar to those obtained for the *Tet* ribozyme by Herschlag and Khosla (1994), with two small differences: the maximum effect of 2′-deoxy substitution seen in the acid pH range is more dramatic for the *Anabaena* ribozyme (2800 for *Anabaena* ribozyme, 600 for *Tet* ribozyme) and the proposed change in the rate-limiting step begins about 1 pH unit higher in the case of the *Anabaena* ribozyme (the apparent pK_a ≃ 6.9 for the *Tet* ribozyme and ≃7.7 for the *Anabaena* ribozyme). Although our results appear to support model 2, this conclusion is preliminary because we have not tested that binding of S and of G unaffected by pH in the range of pH 7−9.

At our standard reaction condition of pH 7.5, the chemical step is largely but not completely rate-limiting for k_{cat} and for $(k_{cat}/K_m)^S$. This is based on two observations: the pH profile (Figure 9) is already leveling off at pH 7.5, and the S/Sd1 cleavage ratio has fallen from its maximum value of 2800 to 1900 (Figure 10). Thus, in studies aimed at measuring the chemical step of the reaction, it is optimal to use pH ≤7.0.

DISCUSSION

We have dissected some of the individual steps involved in catalysis of RNA cleavage by a ribozyme derived from

the *Anabaena* $tRNA^{Leu}$ intron, an efficient self-splicing intron. This intron is much smaller than the *Tetrahymena* intron and differs in 22 of 63 nucleotides within the catalytic core (which consists of P3, P4, P6, P7, and adjacent joining regions; Figure 1). The observed reaction rates for the *Anabaena* ribozyme are very different from those determined previously for the *Tetrahymena* ribozyme: with subsaturating RNA substrate, the rate is more than 10^2 times slower, and with saturating RNA substrate under multiple-turnover conditions, it is more than 10^2 times faster. However, as described below, these differences are a logical consequence of the weaker binding of the RNA substrate by the *Anabaena* ribozyme, which forms a P1 helix of only 3 base pairs. Furthermore, the *Anabaena* and *Tet* ribozymes share some fundamental mechanistic features, including their strength of guanosine binding, stereospecificity with a phosphorothioate at the cleavage site, and log-linear pH−rate profile in the acid pH range. In addition, the rate of the actual chemical cleavage step at neutral pH is within a factor of 6 for the two ribozymes (4−7 min^{-1} for *Anabaena* at 32 °C; ~25 min^{-1} for *Tet* at 30 °C; McConnell et al., 1993). Thus, we conclude that the active sites and the substrate−ribozyme interactions of these two catalytic RNA molecules share some fundamental similarities.

How Tightly Does the Anabaena Ribozyme Bind RNA? The K_m for reaction of the *Anabaena* ribozyme with its cognate oligonucleotide substrate (CUUAAAAA) was measured as 15 ± 2 μM in both single-turnover and multiple-turnover reactions. Considering the simple situation where $K_m = (k_{off} + k_c)/k_{on}$ and the definition $K_d = k_{off}/k_{on}$, then K_m represents the equilibrium dissociation constant K_d only when $k_{off} \gg k_c$ (that is, when RNA substrate S bound in the E·G·S complex is much more likely to dissociate than to react). This is exactly the result obtained in the pulse-chase experiment (Table 2). As a further test, we note that if k_c were contributing significantly to K_m, then K_m would decrease for cleavage of the much less reactive Sd1 substrate, where k_c is much smaller. However, $K_m^{Sd1} = K_m^S$ (Table 4), again providing evidence that $K_m = K_d$. More quantitatively, we estimate that $k_{off} = k_{on}K_d = 10^8\ M^{-1}\ min^{-1} \times 15\ \mu M = 1500\ min^{-1}$, which is clearly much greater than $k_c = k_{cat} = 4\ min^{-1}$. This situation is in marked contrast to that for the *Tet* ribozyme, where studies at 50 °C gave $k_{off} = 0.2\ min^{-1}$, $k_c \simeq 200\ min^{-1}$, and $k_c \gg k_{off}$.

The $K_d^S = 15\ \mu M$ is a remarkably tight binding interaction for a 3 base pair duplex at 32 °C. In terms of standard free energy of formation, this represents a binding interaction of $\Delta G° = RT \ln K_d = -6.7$ kcal/mol. The calculated $\Delta G°$ for the simple duplex

```
5'     C U U A  3'
       | | •
3' C G A G      5'
```

including stabilization for the 3′-overhanging A on the strand analogous to S and the 3′-overhanging C on the strand analogous to the IGS, is only −0.4 kcal/mol (K_d = 0.5 M; Freier et al., 1986). Thus, the ribozyme active site provides additional stabilization estimated as −0.4−(−6.7) = 6.3 kcal/mol, which we attribute to tertiary interactions as yet unidentified. For comparison, direct binding measurements have shown that the *Tet* ribozyme provides 3−4 kcal/mol of tertiary stabilization to the binding of its RNA cleavage product P (Bevilacqua & Turner, 1991; Pyle & Cech, 1991; Herschlag et al., 1993a; Strobel & Cech, 1993), and binding of S occurs with similar net energy (Herschlag & Cech, 1990a; G. Narlikar and D. Herschlag, personal communication). Interestingly, the bulk of the tertiary interactions between the *Tet* ribozyme and its substrate are within the three nucleotides closest to the cleavage site; for the *Anabaena* ribozyme, there are *only* three nucleotides. In addition to the *Anabaena* ribozyme providing a greater amount of tertiary interaction energy for binding S, the locations of the tertiary interactions differ from the *Tet* ribozyme situation (J.A.D.-A. and T.R.C., manuscript in preparation).

Weaker Binding of RNA Accounts for the Different Kinetic Behavior of the Anabaena Ribozyme. In single-turnover reactions with subsaturating RNA substrate [$(k_{cat}/K_m)^S$ conditions], the *Anabaena* ribozyme catalyzes RNA cleavage 10^2 times more slowly than the *Tet* ribozyme. However, as shown in Figure 6, this is a simple consequence of its weaker binding of S. Even if the on-rate for binding of S (the height of the left barrier in Figure 6) and the rate of the chemical step (the height of the right barrier in Figure 6 relative to the energy of E·G·S) were identical for the two ribozymes, the 7 kcal/mol destabilization of the E·G·S ground state for the *Anabaena* ribozyme would by itself account for its smaller $(k_{cat}/K_m)^S$. This is because $(k_{cat}/K_m)^S$ depends on the energy difference between the free components (E·G+S) and the transition state for the highest free-energy barrier, which is the chemical step in the case of the *Anabaena* ribozyme.

Now consider multiple-turnover reactions with saturating RNA substrate [k_{cat}(mt) conditions]. In this case, the *Anabaena* ribozyme catalyzes RNA cleavage 10^2 times more rapidly than the *Tet* ribozyme. Once again, there is a difference in the rate-limiting step: release of cleavage product P is rate-limiting for the *Tet* ribozyme, while the chemical cleavage step is rate-limiting for the *Anabaena* ribozyme. S and P form the same base-pairing interactions with the IGS, so weaker binding of S means similarly weaker binding of P. As calculated above, if k_{off}^P is on the order of 1500 min^{-1} and $k_{cat} = 4\ min^{-1}$, it is clear that the *Anabaena* ribozyme would not have rate-limiting product release. Thus, the *Anabaena* ribozyme cleaves RNA at 4 min^{-1} and quickly releases the products, while the *Tet* ribozyme cleaves RNA very quickly and then releases P at a rate of ~0.01 min^{-1}.

Comparison to Other Ribozymes. We have described the kinetic effects of weakening a ribozyme−substrate interaction going from the *Tet* ribozyme (P1 = 6 bp) to the *Anabaena* ribozyme (P1 = 3 bp). Similar effects have been seen previously when a ribozyme−substrate interaction is weakened in the context of a constant catalytic core.

When a single mismatch is introduced into the P1 interaction of *Tet* ribozyme (at positions other than the conserved G·U at the cleavage site), k_{cat}(mt) increases (Zaug et al., 1988) due to faster product release (Herschlag & Cech, 1990b). Furthermore, under single-turnover conditions, the chemical step becomes at least partially rate-limiting (Herschlag & Cech, 1990b).

A series of hammerhead ribozymes with different numbers of base pairs between the substrate and ribozyme has been studied by Fedor and Uhlenbeck (1992). They found that decreasing the base-pairing energy (e.g., their HH13 → HH8) resulted in a large increase in k_{cat}(mt). Furthermore, most of the HH13-S complex partitions toward cleavage while most of the HH8-S complex dissociates, as judged by pulse−

chase experiments. They describe HH8 as obeying Michaelis–Menten kinetics, characterized by a preequilibrium between E+S and E·S, whereas HH13 is better described by Briggs–Haldane formulation, with cleavage of S occurring more quickly than dissociation of S from the E·S complex. HH8 and HH13 have essentially identical rate constants for the presumed chemical step (Fedor & Uhlenbeck, 1992).

For both the introduction of a mismatch into the *Tet* ribozyme P1 interaction and the weakening of the hammerhead ribozyme–substrate interaction, the catalytic cores were unaltered, so it is not surprising that k_c was not significantly affected. In going from the *Tet* ribozyme to the *Anabaena* ribozyme, which has presumably been selected through evolution to accommodate the shorter P1 helix, it was not obvious that the reaction would respond in a manner so close to that predicted by weakening E·S.

Fundamental Similarities between the Anabaena and Tet Ribozymes. As described above, the difference in affinity for the RNA substrate between these two ribozymes is expected from the different number of base pairs in the substrate–IGS interaction. Furthermore, this difference provides a straightforward explanation of the lower $(k_{cat}/K_m)^S$ and higher k_{cat}(mt) values for the *Anabaena* ribozyme. Underlying these superficial differences are some fundamental similarities, as described below:

(1) Both ribozymes bind G with similar affinity. Binding of pG to the *Tet* ribozyme at 30 °C is characterized by $K_m = 320 \pm 40$ μM, under conditions where $K_m = K_d$ and the measurements represent binding to free E, not E·S (McConnell et al., 1993). Binding of pG to the free *Anabaena* ribozyme has $K_m = 480 \pm 120$ μM, a very similar value. The G-site may be slightly destabilized by removal of the tRNA structure found in the complete pre-tRNA, which shows slightly tighter binding ($K_m = 240 \pm 60$ μM; Zaug et al., 1993). The coupling between RNA substrate binding and G binding seen with the *Tet* ribozyme (McConnell et al., 1993; Bevilacqua et al., 1993) has yet to be studied with the *Anabaena* ribozyme.

(2) Both ribozymes show specificity for the R_P diastereomer of a phosphorothioate introduced at the RNA cleavage site. The *Tet* ribozyme cleaves the R_P diastereomer 2.3-fold more slowly than the normal phosphate-containing substrate (Herschlag et al., 1991), and the *Anabaena* ribozyme has an almost identical thio-effect in the chemical step of its G-dependent transesterification reaction. These modest thio-effects are consistent with rate-limiting chemistry, as shown by comparison with nonenzymatic model reactions (Herschlag et al., 1991). The exceeding slow cleavage seen with the S_P diastereomer by both ribozymes may indicate an important interaction with the *pro*-S_P oxygen atom that is specific to the transition state [Rajagopal et al., 1989; as discussed by Herschlag et al. (1991)].

(3) Both ribozymes cleave an oligonucleotide with a 2′-deoxynucleotide at the cleavage site ~10^3-fold more slowly than an all-RNA substrate. In the case of the *Tet* ribozyme, cleavage rates have been measured with substrates containing 2′-fluoro, 2′,2′-difluoro, and 2′-amino as well as 2′-deoxy substitutions at the cleavage site; the resulting linear free energy relationship indicates that the lower rate with the 2′-deoxy substituent can be largely explained by its providing a less stable leaving group (Herschlag et al., 1993b). The similar magnitude of the deoxy-effect with the *Anabaena* ribozyme is consistent with it also reflecting the inherent greater stability of the deoxyribonucleotide linkage.

The deoxy-effect [k_c(S)/k_c(Sd1)] of 2800 measured for the *Anabaena* ribozyme is greater in magnitude than the value of 600 measured for the *Tet* ribozyme. However, the rate constants for cleavage of S and Sd1 by the *Anabaena* ribozyme both increase with increasing Mg^{2+} concentration, and the S/Sd1 ratio decreases (A.J.Z. and T.R.C., unpublished). Thus, it is not yet clear whether the apparent difference in deoxy-effects between the two ribozymes is significant.

(4) Both ribozymes show log-linear increases in reaction rate with pH in the acid range. [The rate constant that shows this dependence is that which monitors the presumed chemical step: $(k_{cat}/K_m)^S$ or $(k_{cat}/K_m)^G$ for the *Anabaena* ribozyme, $(k_{cat}/K_m)^G$ for the *Tet* ribozyme.] In both cases, the slope of 1 suggests that one proton is lost in the transition state for the chemical step (Herschlag et al., 1993b). Physical models consistent with these data include (a) the 3′-OH of the G nucleophile is deprotonated in the reaction and (b) general base catalysis is provided by a ribozyme group with $pK_a \geq 8$.

(5) Both ribozyme reactions become insensitive to pH in the neutral range, apparently due to a change in the rate-limiting step. In the acid pH range, the actual chemical step is rate-limiting as described in the preceding paragraph. The apparent $pK_a \simeq 7$ reflects a change to a rate-limiting physical step, as evidenced by the decreased effect of deoxy substitution or R_P-phosphorothioate substitution at the cleavage site in the case of the *Tet* ribozyme (Herschlag & Khosla, 1994). For the *Anabaena* ribozyme, the rate effect upon deoxy substitution is also attenuated above pH 7 (Figure 10), consistent with the proposal that a physical step is becoming rate-limiting. The physical step becomes rate-limiting in a single-turnover reaction, so it probably occurs prior to the chemical step. As discussed in detail by Herschlag and Khosla (1994), the specific nature of this step is unknown, but it is likely to be a conformational change.

Although the two ribozymes share many mechanistic features, they also have differences. The greatest difference we have encountered is that the *Anabaena* ribozyme shows no activity in Mn^{2+} (unpublished data), whereas the *Tet* ribozyme has approximately equal activity in Mg^{2+} and Mn^{2+} (Grosshans & Cech, 1989; Piccirilli et al., 1993). Whether this difference is fundamental or represents a fortuitous inhibitory site for Mn^{2+} in the *Anabaena* ribozyme remains to be determined.

Enzymatic Perfection: Three-out-of-Four. The evolution of enzymes toward a state of catalytic perfection has been discussed [for example, see Fersht (1974), Jencks, (1975), and Albery and Knowles (1976)]. Many of the criteria for enzymatic perfection can also be applied to ribozymes, although some—such as the catalyst having a K_m greater than the physiological concentration of substrate—are not relevant to these artifically engineered catalysts. We have therefore focused on four criteria for a "perfect" ribozyme (Herschlag & Cech, 1990b; Young et al., 1991), as follows.

(1) The overall reaction under k_{cat}/K_m conditions should occur as rapidly as base-pairing between ribozyme and substrate. Once this situation is reached, further improvement of the catalytic center which enhances transition state stabilization ceases to be efficacious, because the chemical step is already kinetically invisible. The *Tet* ribozyme meets

this criterion of perfection, with every RNA substrate that is bound undergoing reaction (Herschlag & Cech, 1990b), while the *Anabaena* ribozyme clearly does not: most substrates that are bound are released, not cleaved (Figure 6). Quantitatively, the *Anabaena* ribozyme falls 250−500-fold short of the *Tet* ribozyme.

(2) Products should be rapidly released, so that the ribozyme is not tied up in an E·P complex and multiple-turnover reaction occurs as quickly as the chemical step. This criterion is met by the *Anabaena* ribozyme but not by the *Tet* ribozyme, as already discussed.

(3) Cleavage should occur with high specificity, such that a specific nucleotide sequence is required for cleavage and single-base changes essentially eliminate cleavage. Specificity has not been measured for the *Anabaena* ribozyme, but a prediction can be made with confidence. Having the chemical step occur more slowly than product release allows the binding equilibrium to be established before cleavage. Mismatched substrates will have time to be released before being cleaved. Thus, the *Anabaena* ribozyme should be able to discriminate against a mismatched substrate by an amount equal to the ratio of its K_d to that of the matched substrate. Because the matched substrate binds to the IGS with only 3 base pairs, close to the minimum length for nucleation of a nucleic acid hybrid, the disruption of 1 base pair may be especially destabilizing, thus providing additional specificity for the sequence CUU. In contrast, the *Tet* ribozyme suffers from limited specificity because single-mismatched substrates are cleaved before they can be released (Herschlag & Cech, 1990b). Mutations of the *Tet* ribozyme that destabilize binding of both correct and incorrect sequences can greatly improve specificity (Young et al., 1991).

(4) Cleavage should occur with high fidelity. That is, the correct RNA substrate is cleaved only at a single position, which in the case of a group I ribozyme corresponds to the 5′ splice site (Young et al., 1991). Both the *Tet* and *Anabaena* ribozymes cleave with high fidelity; in fact, we have never observed the *Anabaena* ribozyme to cleave at a site other than the normal CUU/AAAAA, even when cleavage at this position is severely curtailed by deoxyribonucleotide substitution.

In summary, if one evaluates ribozyme perfection in terms of k_{cat}/K_m being limited by substrate base-pairing, multiple turnover being unencumbered by rate-limiting product release, high sequence specificity, and high fidelity of the position of cleavage, then the *Anabaena* ribozyme excels in three-out-of-four criteria.

ACKNOWLEDGMENT

We thank Tim McConnell for preparation of Figure 6, Alice Sirimarco for preparation of the manuscript, and Dan Herschlag for a helpful critique of an earlier draft.

REFERENCES

Albery, W. J., & Knowles, J. R. (1976) *Biochemistry 15*, 5631−5640.

Beaudry, A. A., & Joyce, G. F. (1990) *Biochemistry 29*, 6534−6539.

Benkovic, S. J., & Schray, K. J. (1978) in *Transition States of Biochemical Processes* (Grandour, R. D., Ed.) pp 493−527.

Bevilacqua, P. C., & Turner, D. H. (1991) *Biochemistry 30*, 10632−10640.

Bevilacqua, P. C., Kierzek, R., Johnson, K. A., & Turner, D. H. (1992) *Science 258*, 1355−1358.

Bevilacqua, P. C., Johnson, K. A., & Turner, D. H. (1993) *Proc. Natl. Acad. Sci. U.S.A. 90*, 8357−8361.

Burgers, P. M. J., & Eckstein, F. (1978) *Proc. Natl. Acad. Sci. U.S.A. 75*, 4798−4800.

Burgers, P. M. J., & Eckstein, F. (1979) *Biochemistry 18*, 592−596.

Cech, T. R., Zaug, A. J., & Grabowski, P. J. (1981) *Cell 23*, 467−476.

Cech, T. R., Damberger, S. H., & Gutell, R. R. (1994) *Nature Struct. Biol. 1*, 273−280.

Davanloo, P., Rosenberg, A. H., Dunn, J. J., & Studier, F. W. (1984) *Proc. Natl. Acad. Sci. U.S.A. 81*, 2035−2039.

Davies, R. W., Waring, R. B., Ray, J. A., Brown, T. A., & Scazzocchio, C. (1982) *Nature (London) 300*, 719−724.

Doudna, J. A., & Szostak, J. W. (1989) *Nature (London) 339*, 519−522.

Fedor, M. J., & Uhlenbeck, O. C. (1992) *Biochemistry 31*, 12042−12054.

Fersht, A. R. (1974) *Proc. R. Soc. London, B 187*, 397−407.

Freier, S. M., Kierzek, R., Caruthers, M. H., Neilson, T., & Turner, D. H. (1986) *Biochemistry 25*, 3209−3213.

Griffiths, A. D., Potter, B. V. L., & Eperon, I. C. (1987) *Nucleic Acids Res. 15*, 4145−4162.

Grosshans, C. A., & Cech, T. R. (1989) *Biochemistry 28*, 6888−6894.

Grosshans, C. A., & Cech, T. R. (1991) *Nucleic Acids Res. 19*, 3875−3880.

Herschlag, D. (1992) *Biochemistry 31*, 1386−1399.

Herschlag, D., & Cech, T. R. (1990a) *Biochemistry 29*, 10159−10171.

Herschlag, D., & Cech, T. R. (1990b) *Biochemistry 29*, 10172−10180.

Herschlag, D., & Khosla, M. (1994) *Biochemistry 33*, 5291−5297.

Herschlag, D., Piccirilli, J. A., & Cech, T. R. (1991) *Biochemistry 30*, 4844−4854.

Herschlag, D., Eckstein, F., & Cech, T. R. (1993a) *Biochemistry 32*, 8299−8311.

Herschlag, D., Eckstein, F., & Cech, T. R. (1993b) *Biochemistry 32*, 8312−8321.

Hertel, K. J., Herschlag, D., & Uhlenbeck, O. C. (1994) *Biochemistry 33*, 3374−3385.

Inoue, T., Sullivan, F. X., & Cech, T. R. (1986) *J. Mol. Biol. 189*, 143−165.

Jencks, W. P. (1975) *Adv. Enzymol. Relat. Areas Mol. Biol. 43*, 219−410.

Joyce, G. F., & Inoue, T. (1987) *Nucleic Acids Res. 15*, 9825−9840.

Kay, P. S., & Inoue, T. (1987) *Nature (London) 327*, 343−346.

Knitt, D. S., Narlikar, G. J., & Herschlag, D. (1994) *Biochemistry* (in press).

Kruger, K., Grabowski, P. J., Zaug, A. J., Sands, J., Gottschling, D. E., & Cech, T. R. (1982) *Cell 31*, 147−157.

Kuhsel, M. G., Strickland, R., & Palmer, J. D. (1990) *Science 250*, 1570−1573.

Kunkle, T. A., Roberts, J. D., & Zakour, R. A. (1987) *Methods Enzymol. 154*, 367−382.

McConnell, T. S., Cech, T. R., & Herschlag, D. (1993) *Proc. Natl. Acad. Sci. U.S.A. 90*, 8362−8366.

McSwiggen, J. A., & Cech, T. R. (1989) *Science 244*, 679−683.

Michel, F., & Westhof, E. (1990) *J. Mol. Biol. 216*, 585−610.

Michel, F., Jacquier, A., & Dujon, B. (1982) *Biochimie 64*, 867−881.

Milligan, J. F., Groebe, D. R., Witherell, G. W., & Uhlenbeck, O. C. (1987) *Nucleic Acids Res. 15*, 8783−8798.
Piccirilli, J. A., Vyle, J. S., Caruthers, M. H., & Cech, T. R. (1993) *Nature (London) 361*, 85−88.
Pyle, A. M., & Cech, T. R. (1991) *Nature 350*, 628−631.
Pyle, A. M., & Green, J. B. (1994) *Biochemistry 33*, 2716−2725.
Pyle, A. M., Murphy, F. L., & Cech, T. R. (1992) *Nature (London) 358*, 123−128.
Rajagopal, J., Doudna, J. A., & Szostak, J. W. (1989) *Science 244*, 692−694.
Rose, I. A., O'Connell, E. L., Litwin, S., & Bar Tana, J. (1974) *J. Biol. Chem. 249*, 5163−5168.
Saldanha, R., Mohr, G., Belfort, M., & Lambowitz, A. M. (1993) *FASEB J. 7*, 15−24.
Salvo, J. L., & Belfort, M. (1992) *J. Biol. Chem. 267*, 2845−2848.
Strobel, S. A., & Cech, T. A. (1993) *Biochemistry 32*, 13593−13604.
Symons, R. H. (1992) *Annu. Rev. Biochem. 61*, 595−605.
Tanner, N. K., & Cech, T. R. (1987) *Biochemistry 26*, 3330−3340.
Turner, D. H., Sugimoto, N., & Freier, S. M. (1990) in *Nucleic Acids*, Vol. 1c, Landolt-Bornstein series (Saenger, W., Ed.) pp 201−227, Springer-Verlag, Berlin.
Van der Horst, G., Christian, A., & Inoue, T. (1991) *Proc. Natl. Acad. Sci. U.S.A. 88*, 184−188.
Xu, M. Q., Kathe, S. D., Goodrich-Blair, H., Nierzwicki-Bauer, S. A., & Shub, D. A. (1990) *Science 250*, 1566−1570.
Young, B., Herschlag, D., & Cech, T. R. (1991) *Cell 67*, 1007−1019.
Zaug, A. J., & Cech, T. R. (1982) *Nucleic Acids Res. 10*, 2823−2838.
Zaug, A. J., Kent, J. R., & Cech, T. R. (1984) *Science 224*, 575−578.
Zaug, A. J., Been, M. D., & Cech, T. R. (1986) *Nature (London) 324*, 429−433.
Zaug, A. J., Grosshans, C. A., & Cech, T. R. (1988) *Biochemistry 27*, 8924−8931.
Zaug, A. J., McEvoy, M. M., & Cech, T. R. (1993) *Biochemistry 32*, 7946−7953.